Structural characterization of the metal/glass interface in bioactive glass coatings on Ti-6Al-4V

T. OKU, K. SUGANUMA, L. R. WALLENBERG
Institute of Scientific and Industrial Research, Osaka University, Osaka 567–0047, Japan
E-mail: Oku@sanken.osaka-u.ac.jp

A. P. TOMSIA, J. M. GOMEZ-VEGA, E. SAIZ
Lawrence Berkeley National Laboratory, Berkeley CA 94720, USA

Coating Ti-based implants with bioactive materials promotes joining between the prostheses and the bone as well as increasing long-term implant stability. In the present work, the interface between Ti-6Al-4V and bioactive silicate glass coatings, prepared using a simple enameling technique, is analyzed. High-resolution transmission electron microscopy of the glass/alloy interface shows the formation of a reaction layer ($\sim$ 150 nm thick) composed of Ti_5Si_3 nanoparticles with a size of $\sim$ 20 nm. This nanostructured interface facilitates the formation of a stable joint between the glass coating and the alloy.

1. Introduction

Ti and Ti-based alloys are widely used in the fabrication of prosthetic implants. Since the implant life is strongly dependent on the strength of their attachment to the bone, implants are often coated with a hydroxyapatite (HA) layer in order to promote adhesion. Synthetic HA, $Ca_{10}(PO_4)_6(OH)_2$, is bioactive [1, 2] and similar in structure and composition to the mineral component of the bone. High-resolution microscopy studies have shown that HA can attach epitaxially to the bone [3]. The most commonly used techniques to fabricate HA coating are plasma-spraying and ion sputtering. Plasma-spraying produces porous coatings with thickness ranging between 50 to 200 μm. However, HA changes in chemical composition and crystal structure during the plasma process [4, 5], and the final coatings do not adhere well to the metal [6]. Ion sputtering produces very thin ($\sim$ 1 μm) and dense HA layers that lack open porosity, hindering the desired osseointegration. Both techniques are ''line of sight'' methods not suitable for coating complicated shapes.

A new method to fabricate bioactive coatings on Ti and Ti-based alloys, using glasses in the system SiO_2-Na_2O-K_2O-CaO-MgO-P_2O_5, was developed in a previous work [7–9]. The composition of the glasses was derived from the Bioglass® originally developed by Hench [10] by increasing the SiO_2 content, then, partially substituting K_2O for Na_2O and MgO for CaO. The objective was to reduce the coefficient of thermal expansion (α) of Bioglass® ($14 \times 10^{-6}\,°C^{-1}$) [11] and make it compatible with that of Ti or Ti-6Al-4V (at 400 °C, $\alpha_{Ti6Al4V} \approx 9.1 - 9.8 \times 10^{-6}\,°C^{-1}$; $\alpha_{Ti} \approx 9.4 \times 10^{-6}\,°C^{-1}$ [12]). Using these glasses, it has been possible to fabricate coatings with thickness ranging between 25 and 150 μm, that showed good adhesion to the metal and formed HA crystals on their surface after soaking for 30 days in simulated body fluid at 36–37 °C [8–9]. In order to design and control the interface between the glasses and the Ti alloys, we must understand their bonding mechanism, which requires analysis of the interfacial microstructure at the nanoscopic scale.

The purpose of the present work is to analyze the bioglass/Ti-6Al-4V interface formed during enameling. To understand the nature of the interfaces that presented optimum adhesion, microstructural analysis was carried out by high-resolution electron microscopy (HREM), a powerful method for structural analysis of advanced materials at the atomic scale [13–15]. These studies will provide a guideline for designing and controlling the interfaces between Ti alloys and bioactive glass coatings that can be used in future prosthetic implants.

2. Experimental procedures

A glass in the SiO_2-Na_2O-K_2O-CaO-MgO-P_2O_5 system was prepared starting from silica powder (99.9%) and reagent grade $CaCO_3$, $NaPO_3$, Na_2CO_3, K_2CO_3 and MgO. The composition of the glass, denominated 6P57, is (in wt %): SiO_2, 56.5; Na_2O, 11.0; K_2O, 3.0; CaO, 15.0; P_2O_5, 8.5; P_2O_5, 6.0. The glass was synthesized by mixing the ingredients in ethanol using a high-speed stirrer. After drying in air (12 h at 80 °C), the powder mixture was fired in a Pt crucible for 4 h at 1400 °C and the melt was cast in a graphite mold.

To prepare the glass coatings, glass powder with particle size < 30 μm was first obtained by grinding glass pellets in a planetary mill with agate balls. A suspension of the powder in ethanol was then deposited over Ti-6Al-4V plates (99% purity, $15 \times 10 \times 1$ mm), which had been previously polished with 1 μm diamond paste and cleaned in acetone and ethanol. The samples

were then fired in air in a Unitek dental furnace. The coatings were introduced into the preheated to 600 °C furnace and subsequently heated at 40 °C/min up to 800 °C. This temperature was maintained for 30 s, and afterwards the samples were quenched in air. During heating, the oven was evacuated to 1.3×10^{-5} Pa. Once the maximum temperature was reached, the vacuum was released. This firing condition yields 6P57 coatings on Ti-6Al-4V with optimum adhesion [7–9]. The final coating thickness was $\sim 50\,\mu$m.

Cross-sections of the glass/Ti-6Al-4V interface were analyzed by electron probe micro analysis (EPMA) in micron scale. Samples for HREM were prepared by cutting cross-sections of the glass/Ti-6Al-4V interface. The sections were ground to a thickness of $\sim 100\,\mu$m with emery paper, and then fixed into a Cu mesh with 3 mm diameter. The discs were polished with a dimple grinder (Gatan, Model 656) to less than 20 μm in thickness and milled by argon ion-milling (E.A. Fischione Instruments, Inc., Model 3000) at an accelerating voltage of 2 to 4 kV. HREM observations were performed with a 1250 kV electron microscope (ARM-1250 kV) having a point-to-point resolution of 0.12 nm. Negative films were converted into digital data using a film scanner (AGFA, Select Scan Scan Plus) and printed in a Pictrography 3000 printer (Film Co. Ltd).

3. Results and discussion

An EPMA image and line profiles of the elements at the glass/Ti-Al-V interface annealed at 800 °C for 30 s are shown in Fig. 1 (a) and (b), respectively. The interface is smooth and stable In micron scale, and no special diffusion was observed at the interface.

A low-magnification image and an electron diffraction pattern of the 6P57/Ti-6Al-4V interface annealed at 800 °C for 30 s is shown in Fig. 2. Titanium alloys are single crystals in micron scale, and only two reflections corresponding to 100 of the Ti are observed in the diffraction pattern. A diffuse ring of SiO_2 100 is observed as indicated by arrows. Many diffraction spots due to Ti_5Si_3 polycrystals are observed. In the image, a titanium silicide (Ti_5Si_3) layer, ~ 150 nm thick, can be observed at the interface. The Ti_3Si_3 layer is divided into two regions: a continuous nanocrystalline layer in contact with the alloy and, on top of it, a zone with isolated Ti_5Si_3 nanoparticles dispersed in the glass. The appearance of isolated particles on the transmission electron microscope (TEM) image can also result from the growth of elongated silicide grains, or dendrites, from the continuous layer into the glass. Consequently, they may appear as isolated particles (in the TEM samples) wherever the dendrite intersects the cross-section.

An enlarged HREM image of Fig. 2 is shown in Fig. 3. Fig. 3 (a) corresponds to the Ti_5Si_3/alloy interface, where the lattice fringes of Ti $\{1\,0\,0\}$ and $Ti_5Si_3\{1\,2\,1\}$ are visible. A good lattice match exists between them, which can help in obtaining good adhesion. The glass/Ti_5Si_3 interface is shown in Fig. 3 (b). The size of the particles is in the range of ~ 20 nm, and Ti_5Si_3 lattice fringes can be observed ($\{1\,2\,0\}$, $\{0\,1\,0\}$ and $\{0\,1\,2\}$). Fig. 4 is an HREM image of a Ti_5Si_3 nanoparticle in the bioglass away from the continuous Ti_5Si_3 layer.

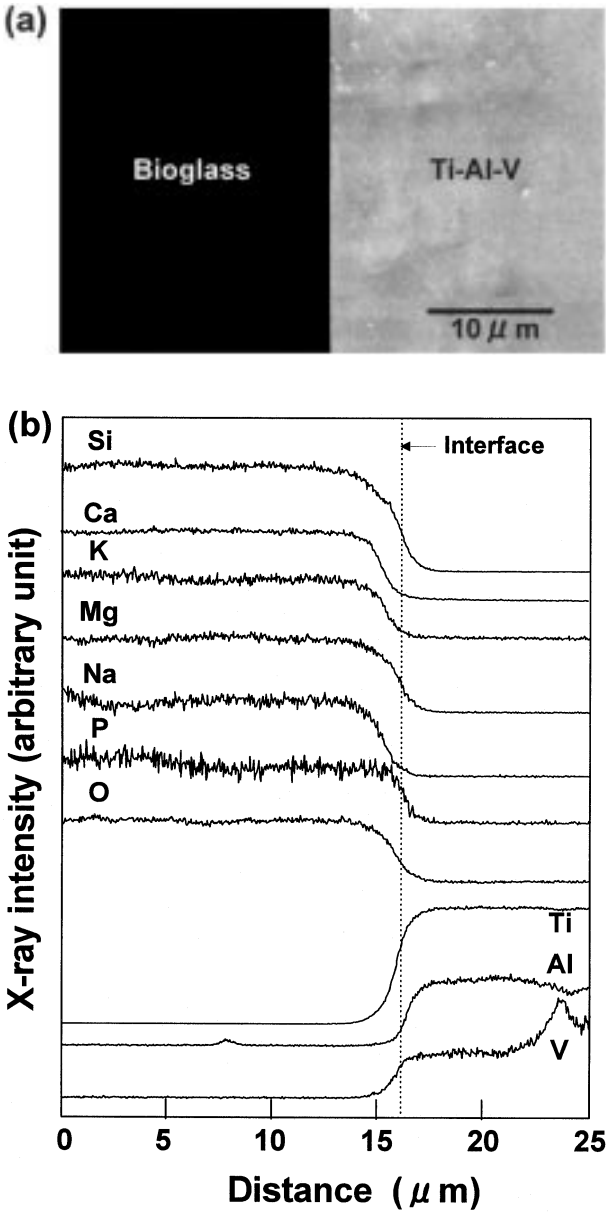

Figure 1 (a) EPMA image of the cross-section of a glass coating on Ti-6Al-4V annealed at 800 °C for 30 sec. (b) Line profiles of the elements near the interface.

The evolution of the glass/metal interfacial nanostructure, deduced from the HREM observations, is schematically illustrated in Fig. 5. Thin-film X-ray diffraction showed the presence of a TiO_x layer on substrates annealed at temperatures below the glass softening point (637 °C) [7–9]. During heating, oxygen gas easily diffuses through the porous deposited glass coating and a thin oxide layer forms on the surface of the titanium alloy. At temperatures higher than the softening point of the glass, the glass layer flows and sinters. The inner glass/metal interface becomes sealed from the external atmosphere, and the glass dissolves the TiO_X layer and starts to react with the substrate. HREM shows the formation of a ~ 150 nm silicide layer after annealing at 800 °C for 30 s. Coatings fired under these conditions do not delaminate when indentations up to 6.2 kg are made on their surface

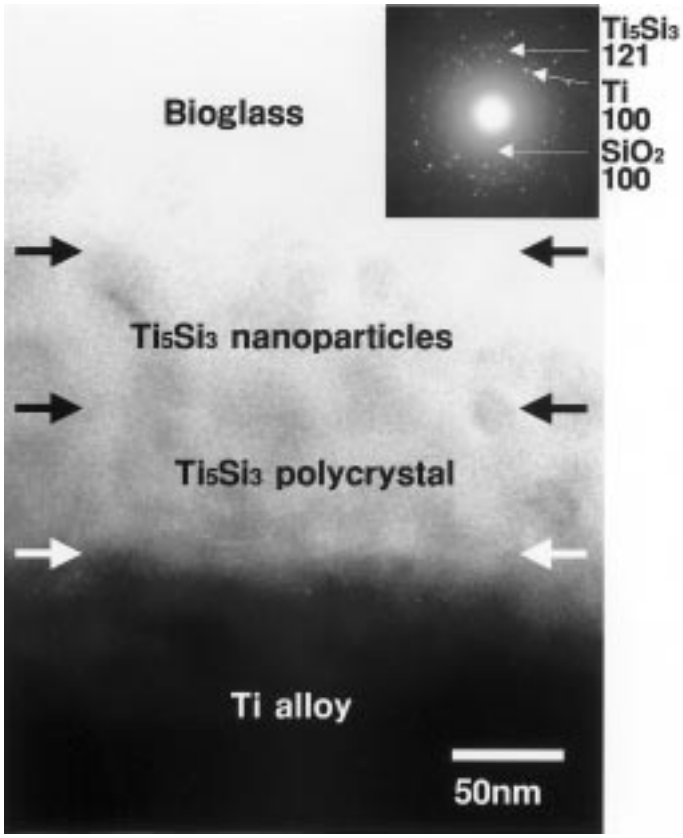

Figure 2 Low magnification image and electron diffraction pattern of the cross-section of a glass coating on Ti-6Al-4V annealed at 800 °C for 30 sec.

[9]. Ti_5Si_3 was also detected by X-ray diffraction in samples annealed at 850 °C for 60 s [7–9]. The formation of silicides occurs according to the following reaction

$$Ti + 3SiO_2\{glass\} \rightarrow Ti_5Si_3 + 3O_2\{gas\} \qquad (1)$$

Excessive reaction and the formation of silicides are undesirable to establish a good ceramic/metal interface. Silicides are usually brittle and have higher thermal expansion coefficient ($\alpha_{Ti}5_{si}3 = 11.1 \times 10^{-6}\ °C^{-1}$ [16]) than Ti-6Al-4V. Also, the liberation of oxygen gas (reaction [1]) will eventually result in the formation

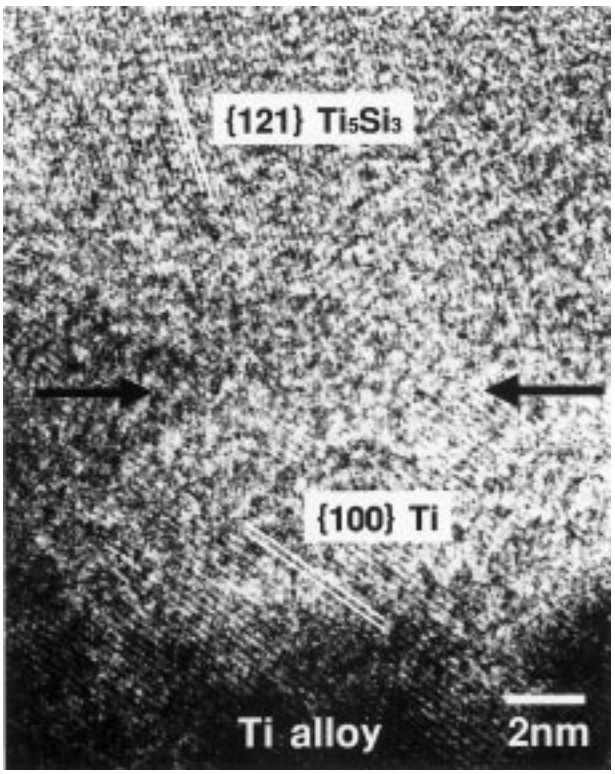

(a)

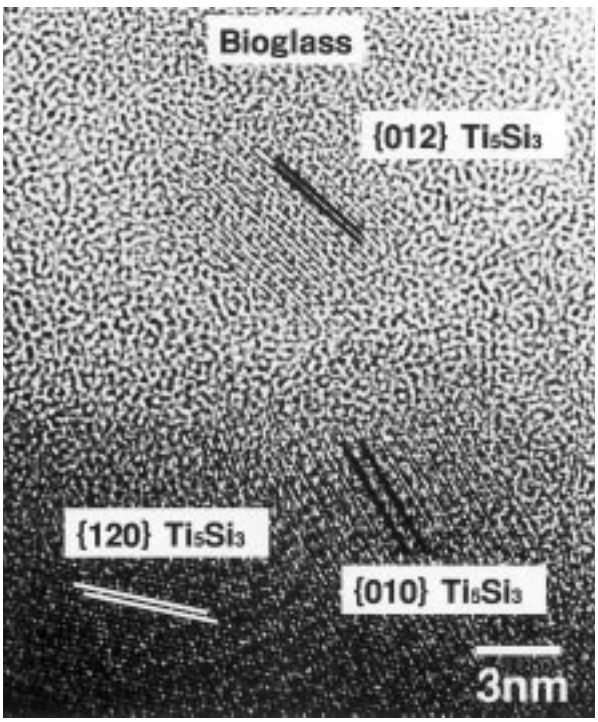

(b)

Figure 3 HREM image of (a) the Ti_5Si_3/Ti-6Al-4V interface, and (b) the 6P57/Ti_5Si_3 interface formed after annealing at 800 °C for 30 sec.

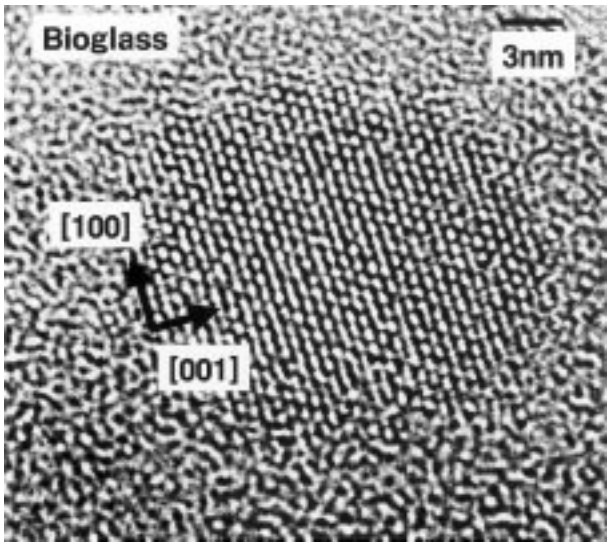

Figure 4 HREM image of a Ti_5Si_3 nanoparticle in bioglass formed after 30 sec at 800 °C.

of bubbles in the coating. On the other hand, a thick oxide layer remaining at the interface results in weak bonding resulting from porosity in the oxide and its physical incompatibility with the metal.

According to conventional enameling theory, in order to achieve optimum glass/metal bonding, the glass should be saturated with the lowest valence oxide of the metal with no any interfacial layer. In this way, according to the theory, a transition region will form between the metallic bonding of the substrate and the ionocovalent bonding of the glass, providing a ''continuity of electronic structure'' that will result in good adhesion [17]. However, the lack of characterization of enamel interfaces at the atomic level precludes a complete confirmation of this theory. More recent analysis of metal/oxide interfaces try to explain bonding in terms of fundamental contributions of image (electrostatic) forces and localized atomic bonding [18]. In this work, HREM of the interface for coatings with optimum adhesion has shown the presence of a thin Ti_5Si_3 interfacial layer. It is proposed that a strong bond forms between the thin silicide layer and the metal, helped in part by the good lattice matching, and that the nanostructured interface provides some strain relaxation that can improve bonding. Also, if Ti_5Si_3 dendrites grow into the glass, they can provide some mechanical interlocking that can contribute to the adhesion. Control of the interfacial reaction is an important factor

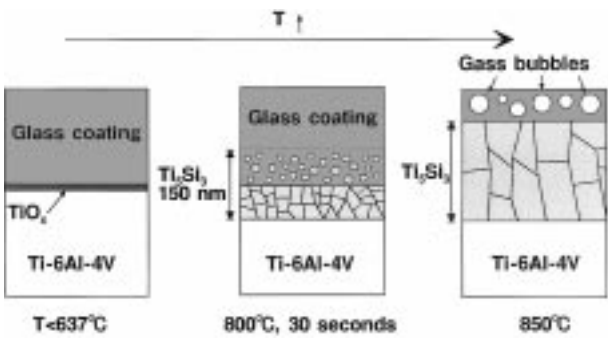

Figure 5 Schematic illustration of the glass/alloy interface evolution during firing.

in these materials, and care must be taken to prevent excessive reaction which can result in loss of adhesion due to the formation of a thick silicide layer accompanied by bubbles in the glass.

In a previous work, it was shown that control of the reactivity between the glass and Ti was impossible when the coatings where fired in an inert atmosphere [8]. In air, oxidation of the alloy substrate during heating provides a temporary buffer between glass and metal that allows the glass to flow and densify without redox interfacial reactions.

4. Summary

The interfacial structure between Ti-6Al-4V alloy and bioactive glass coatings prepared using an enameling technique was investigated by HREM. In coatings fired under the optimum conditions, reaction between the SiO_2 in the glass and Ti resulted in the formation of a thin Ti_5Si_3 layer ($\sim$ 150 nm thick) at the glass/alloy interface. The Ti_5Si_3 layer divided into two regions: a continuous nanocrystalline layer in contact with the alloy and a zone with isolated Ti_5Si_3 nanoparticles dispersed in the glass. The diameter of the silicide particles was $\sim$ 20 nm. Formation of a nanostructured interface helped bonding by facilitating strain relaxation at the interface. Control of the interfacial reaction between the glass and the Ti-based alloys was crucial. The formation of the thin silicide layer resulted in stable and strong adhesion, but if a thin TiO_X layer remained at the interface or the reaction was excessive, the coatings were weak and easily delaminate.

Acknowledgment

The authors would like to acknowledge Professor K. Hiraga and Mr E. Aoyagi for allowing us to use the electron microscope. This work is partly supported by The COE (Center of Excellence) Program, Ministry of Education, Science, Sports and Culture, Japan, and the NIH/NIDR grant 1R01DE11289 at LBNL.

References

1. K. DONATH, in ''Osseo-Integrated Implants Vol. 1'' edited by G. Heimke, (CRC Press, Boca Raton, FL, 1990) p. 99.
2. J. F. KAY, *Dent. Clin. North. Am.* **36** (1992) 1.
3. W. BONFIELD and Z. B. LUKLINSKA, in ''The Bone-Biomaterial Interface'' edited by J. E. Davies (University of Toronto Press, 1991) p. 89.
4. J. L. ONG, L. C. LUCAS, W. R. LACEFIELD and E. D. RIGNEY, *Biomaterials* **13** (1992) 249.
5. K. DE GROOT, *The Cent. Mem. Ist. Ceram. Soc. Jap.* **99** (1991) 943.
6. G. W. HASTINGS, D. DAILLY and S. MORREY, in ''Bioceramics, Vol. 1'' edited by H. Ohnishi, H. Aoki and K. Sawai (Ishiyaku EuroAmerica, 1989) p. 355.
7. A. PAZO, E. SAIZ and A. P. TOMSIA, *Acta Mater.* **46** (1998) 2551.
8. A. PAZO, E. SAIZ and A. P. TOMSIA, in ''Ceramic Microstructures'', edited by A. P. Tomsia and A. M. Glaeser (Plenum Press, New York, 1998) p. 543.
9. J. M. GOMEZ-VEGA, E. SAIZ and A. P. TOMSIA, *J. Biomed. Mater. Res.*, submitted.
10. L. L. HENCH, in ''Bioceramics: Material Characteristics Versus In Vivo behavior'' edited by P. Ducheyne and J. E. Lemmons, (Annals of the New York Academy of Sciences, Vol. 523, New York, 1988).

11. A. KRAJEWSKI, A. RAVAGLIOLI, G. DE PORTU and R. VISANI, *Am. Ceram. Soc. Bull.* **64** (1985) 679.
12. ''Metals Handbook, 9th edition, Vol. 3'' (American Society for Metals, Metals Park, Ohio, 1980) p. 372.
13. T. OKU and S. NAKAJIMA, *J. Mat. Res.* **13** (1998) 1136.
14. T. OKU, A. CARLSSON, L. R. WALLENBERG, J.-O. MALM, J.-O. BOVIN, I. HIGASHI, T. TANAKA, Y. ISHIZAWA, *J. Sol. St. Chem.* **135** (1998) 182.
15. T. OKU and S. NAKAJIMA, *Appl. Phys. Lett.* **75** (1999) 4266.
16. V. S. NESHPUR and M. I. REZNICHENKO, *Refractories* **28** (1963) 145.
17. J. A. PASK, *Ceram. Bull.* **66** (1987) 1587.
18. M. W. FINNIS, *J. Phys.: Cond. Mat.* **8** (1996) 5811.

Received 21 April
and accepted 15 December 1999